Nonlinear screening of spherical and cylindrical colloids: The case of 1:2 and 2:1 electrolytes

Gabriel Téllez*
Departamento de Física, Universidad de Los Andes, A.A. 4976, Bogotá, Colombia

Emmanuel Trizac†
Laboratoire de Physique Théorique (Unité Mixte de Recherche UMR 8627 du CNRS), Bâtiment 210, Université de Paris–Sud, 91405 Orsay Cedex, France

(Received 16 March 2004; published 26 July 2004)

From a multiple scale analysis, we find an analytic solution of spherical and cylindrical Poisson-Boltzmann theory for both a 1:2 (monovalent coions, divalent counterions) and a 2:1 (reversed situation) electrolyte. Our approach consists of an expansion in powers of rescaled curvature $1/(\kappa a)$, where a is the colloidal radius and $1/\kappa$ the Debye length of the electrolytic solution. A systematic comparison with the full numerical solution of the problem shows that for cylinders and spheres, our results are accurate as soon as $\kappa a > 1$. We also report an unusual overshooting effect where the colloidal effective charge is larger than the bare one.

DOI: 10.1103/PhysRevE.70.011404 PACS number(s): 82.70.Dd, 61.20.Gy

I. INTRODUCTION

Almost a century ago, the work of Gouy [1], followed by that of Chapman [2], established the foundations of the mean-field treatment of the electric double layer (Poisson-Boltzmann theory). This approach served as a basis for computing microionic correlations in a homogeneous electrolyte [3], and later led to the prominent DLVO theory of colloidal interactions [4]. An essential notion in this context is that of charge renormalization [5–9]: at large distances, the electrostatic signature of a charged body (with charge $Z_{\rm bare}$) in an electrolyte takes the same form as that of an effective macroion with a suitable effective charge $Z_{\rm eff}$, the latter object being treated within linearized Poisson-Boltzmann theory. Only for small $Z_{\rm bare}$ do effective and bare parameters coincide (weak coupling limit). In general, one has $|Z_{\rm eff}| \ll |Z_{\rm bare}|$, which reflects the nonlinear screening effect of the electric double layer around a colloid [10]. This nonlinear regime, beyond the weak coupling limit but below the couplings that would invalidate the mean-field assumption underlying the approach, is precisely that which is relevant for colloids (see, e.g., the discussion in Refs. [7,11]).

Recently, analytical expressions have been obtained, within Poisson-Boltzmann theory, for the effective charges of spherical and cylindrical macroions [12]. These predictions for a unique macroion, immersed in an infinite sea of monovalent electrolyte with inverse Debye length κ, are exact up to $(\kappa a)^{-1}$ corrections, where a is the radius of the macroion. For practical purposes, the predictions are accurate as soon as $\kappa a > 1$. In this paper, we consider the situation of spherical and cylindrical macroions in a charge asymmetric electrolyte with both monovalent and divalent microions. The asymmetry of electrolyte has noticeable consequences on the structure of the electric double layer, and the case of 2:1 electrolytes (i.e., with divalent coions and monovalent counterions) turns out to differ much from the 1:2 situation (monovalent coion, divalent counterion). Our analytical results—obtained from a multiple scale technique [13]—neglect $O(\kappa a)^{-2}$ corrections for the electrostatic potential and, conversely, $O(\kappa a)^{-1}$ terms for effective charges. By an explicit comparison with the numerical mean-field results, they will be shown to be precise whenever $\kappa a > 1$, as was the case in Ref. [12]. In Sec. II the general method will be presented, and the electrostatic potential obtained. The results concerning effective quantities will be given in Secs. III and IV. Conclusions will be drawn in Sec. V.

II. QUASIPLANAR SOLUTION TO POISSON-BOLTZMANN EQUATION FOR 2:1 OR 1:2 ELECTROLYTES

A. 2:1 electrolyte

We consider a cylindrical ($j=1$) or spherical ($j=2$) colloid of radius a with surface charge density $e\sigma > 0$ immersed in an electrolyte with coions (respectively, counterions) of valency z_1 (respectively, z_2) and numeric density n_1 (respectively, n_2). Let us analyze in some detail the case $z_1=2$, $z_2=-1$, hereafter referred to as 2:1.

As usual, we define the Debye length $\kappa^{-1} = (4\pi l_B \Sigma_i n_i z_i^2)^{-1/2} = (12\pi n_2 l_B)^{1/2}$, the reduced electrical potential $y = \beta e \psi$, and $\sigma^* = 4\pi l_B \sigma a$. Here, l_B denotes the Bjerrum length, defined from the permittivity χ of the suspending medium and the inverse temperature $\beta = 1/(kT)$ as $l_B = \beta e^2/\chi$. Using the method of multiple scales, closely following Ref. [13], the Poisson-Boltzmann equation

$$\frac{1}{r^j}\frac{d}{dr}\left[r^j \frac{dy}{dr}\right] = -4\pi l_B n_2 (e^{-2y} - e^{y}), \tag{2.1}$$

can be cast into

$$\frac{\partial^2 y}{\partial x_1^2} + \frac{2\epsilon \partial^2 y}{\partial x_1 \partial x_2} + \frac{\epsilon j}{x_2}\frac{\partial y}{\partial x_1} + \epsilon^2 \frac{\partial^2 y}{\partial x_2^2} + \frac{\epsilon^2 j}{x_2}\frac{\partial y}{\partial x_2} = -\frac{1}{3}(e^{-2y} - e^{y}), \tag{2.2}$$

with boundary conditions

*Electronic address: gtellez@uniandes.edu.co
†Electronic address: emmanuel.trizac@th.u-psud.fr

$$\left[\frac{\partial y}{\epsilon\partial x_1}+\frac{\partial y}{\partial x_2}\right]_{x_1=0,x_2=1}=-\sigma^*, \tag{2.3a}$$

$$\lim_{x_1\to\infty,x_2\to\infty} x_2^j\left[\frac{\partial y}{\epsilon\partial x_1}+\frac{\partial y}{\partial x_2}\right]=0. \tag{2.3b}$$

Here, we have defined $\epsilon=(\kappa a)^{-1}$, $x_1=\kappa(r-a)$, and $x_2=r/a$. We seek a solution as an expansion in powers of ϵ which is supposed to be a small parameter: $y=y_0+\epsilon y_1+\cdots$.

The equation for the zeroth-order term is the Poisson-Boltzmann equation for a planar interface

$$\frac{\partial^2 y_0}{\partial x_1^2}=-\frac{1}{3}(e^{-2y_0}-e^{y_0}), \tag{2.4}$$

which was solved by Gouy in his pioneering work [1] (see also Grahame [14]). The solution reads

$$y_0(x_1,x_2)=\ln\left(1+\frac{6q}{(1-q)^2}\right), \tag{2.5}$$

with the shorthand notation $q=t(x_2)e^{-x_1}$, which will be used extensively in the following. Here, $t(x_2)$ is a function of x_2 which appears as a constant of integration (with respect to x_1), since in Eq. (2.4) the variable x_2 does not appear. As explained in Ref. [13], this function is determined by the requirement that the nonhomogeneous part of the differential equation for the next order, y_1, decays faster than e^{-x_1} when $x_1\to\infty$. The equation for y_1 reads

$$\frac{\partial^2 y_1}{\partial x_1^2}-\frac{1}{3}(2e^{-2y_0}+e^{y_0})y_1=-\frac{2\partial^2 y_0}{\partial x_1\partial x_2}-\frac{j}{x_2}\frac{\partial y_0}{\partial x_1}. \tag{2.6}$$

The requirement that the right-hand side of Eq. (2.6) decay faster than e^{-x_1} leads to $t(x_2)=Ax_2^{-j/2}$, with A a constant of integration. We therefore have

$$q=Ax_2^{-j/2}e^{-x_1}. \tag{2.7}$$

Notice that the situation is exactly the same as in the 1:1 electrolyte case[13]; the zero-order solution in the quasiplanar approximation is obtained from the planar solution with the replacement of the constant of integration A by $Ax_2^{-j/2}$. Actually, this is a general result for any type of electrolyte, since the right-hand side of Eq. (2.6) does not depend on the microscopic constitution of the electrolyte, and when $x_1\to\infty$ for any electrolyte the behavior of y_0 will be given by the Debye-Hückel solution: $\mathrm{cst}\times t(x_2)\exp(-x_1)$.

The constant of integration A can be expressed as a function of the surface charge density σ^* by enforcing the boundary condition (2.3a) at the dominant order

$$\left.\frac{\partial y_0}{\partial x_1}\right|_{x_1=0,x_2=1}=-s, \tag{2.8}$$

where we have set $s=\epsilon\sigma^*$. This gives a third-order equation for A

$$\frac{6A(1+A)}{(1-A)(A^2+4A+1)}=s. \tag{2.9}$$

Its physical solution (which vanishes when $s\to 0$) can be written as

$$A=\frac{1}{s}\left[-2-s+2^{3/2}(2+s+s^2)^{1/2}\cos\left(\frac{\theta}{3}\right)\right], \tag{2.10}$$

with

$$\theta=\cos^{-1}\left[\frac{-4-3s-3s^2-s^3}{\sqrt{2}(2+s+s^2)^{3/2}}\right]. \tag{2.11}$$

This constant has also been computed in the study of the planar interface effective charge ($6A=4\pi s_{\mathrm{eff}}$) in Ref. [15], although it is presented there in a slightly different (but completely equivalent) form.

Replacing the explicit expression (2.5) for y_0 into Eq. (2.6) gives for the order-one term y_1 the following equation:

$$\frac{\partial^2 y_1}{\partial x_1^2}-\frac{1+27q^2+16q^3+27q^4+q^6}{(1-q)^2(1+4q+q^2)^2}y_1 =-\frac{12j}{x_2}\frac{q^2(q^3+3q^2+3q-1)}{(1-q)^2(1+4q+q^2)^2}. \tag{2.12}$$

Using the variable q instead of x_1 and performing the change of function $y_1(x_1,x_2)=f(q)/[(1-q)(1+4q+q^2)]$ yields a second-order linear differential nonhomogeneous equation for $f(q)$ with polynomial coefficients in q whose associated linear homogeneous equation has the simple solution $f(q)=q(q+1)$, therefore allowing the complete solution of the nonhomogeneous equation to be found using the traditional method of "variation of the constant." After some tedious but otherwise straightforward calculations, we find the solution satisfying the appropriate boundary condition (2.3b) at infinity

$$y_1(x_1,x_2)=\frac{k(x_2)q(q+1)-\dfrac{j}{2x_2}q^2(q^2+9q-8)}{(1-q)(1+4q+q^2)}. \tag{2.13}$$

Again, there is a function $k(x_2)$ that appears as a constant of integration with respect to x_1 since there are no derivatives of y_1 with respect to x_2 in Eq. (2.6). This function $k(x_2)$ is determined [13] by the requirement that the nonhomogeneous part of the equation for the next order term y_2 decreases faster than e^{-x_1} when $x_1\to\infty$

$$\frac{\partial^2 y_0}{\partial x_2^2}+\frac{j}{x_2}\frac{\partial y_0}{\partial x_2}+2\frac{\partial^2 y_1}{\partial x_1 \partial x_2}+\frac{j}{x_2}\frac{\partial y_1}{\partial x_1}+y_1^2(e^{y_0}-4e^{-2y_0})=o(e^{-x_1}). \tag{2.14}$$

This gives $k(x_2)=c_1+3j(j-2)/(4x_2)$, with c_1 another constant of integration, so finally the order-one solution is

$$y_1(x_1,x_2)=\frac{[c_1+\frac{3j(j-2)}{4x_2}]q(q+1)-\frac{j}{2x_2}q^2(q^2+9q-8)}{(1-q)(1+4q+q^2)}. \tag{2.15}$$

Applying the boundary condition (2.3a) to the next order in ϵ gives the equation $\partial_{x_1}y_1+\partial_{x_2}y_0|_{x_1=0,x_2=1}=0$, and subsequently determines the constant of integration

$$c_1=-j\frac{2A^6+12A^5+A^4(34+3j)+2A^3(-88+3j)+6A^2(-7+3j)+2A(34+3j)+3(2+j)}{4(1+2A+6A^2+2A^3+A^4)}. \tag{2.16}$$

The quantity A is given by Eq. (2.10). Both constants A and c_1 are related to the effective charge of the colloid and therefore carry important physical information about the system. Let us notice that at saturation $\sigma\to\infty$, they take simple values: $A^{\mathrm{sat}}=1$ and $c_1^{\mathrm{sat}}=-j(3j-8)/4$.

B. 1:2 electrolyte

The quasiplanar approximate solution of the Poisson-Boltzmann equation for the case $z_1=1$ and $z_2=-2$ (1:2 electrolyte) follows from similar calculations. We only report the results. The zero-order term y_0 reads

$$y_0(x_1,x_2)=-\ln\left(1-\frac{6q}{(q+1)^2}\right), \tag{2.17}$$

with q given by Eq. (2.7), and the order-one term is

$$y_1(x_1,x_2)=\frac{-q(q-1)[c_1+\frac{3j(j-2)}{4x_2}]+\frac{j}{2x_2}q^2(q^2-9q-8)}{(1+q)(1-4q+q^2)}. \tag{2.18}$$

Note that the solution for the 1:2 case is simply obtained from the one for the 2:1 case by a global change of sign and by replacing q by $-q$.

The constant of integration A is again a solution of a third-order equation which can be obtained from Eq. (2.9) by a global change of sign and by replacing A by $-A$. However, the physical solution is not the same as in the 2:1 case, and now takes the form

$$A=\frac{1}{s}\left[-2+s+2^{3/2}(2-s+s^2)^{1/2}\cos\left(\frac{\theta+4\pi}{3}\right)\right], \tag{2.19}$$

with θ given by

$$\theta=\cos^{-1}\left[\frac{-4+3s-3s^2+s^3}{\sqrt{2}(2-s+s^2)^{3/2}}\right]. \tag{2.20}$$

The constant of integration for the order-one term is here

$$c_1=-j\frac{2A^6-12A^5+A^4(34+3j)-2A^3(-88+3j)+6A^2(-7+3j)-2A(34+3j)+3(2+j)}{4(1-2A+6A^2-2A^3+A^4)}, \tag{2.21}$$

with A given by Eq. (2.19). The saturation ($s\to\infty$) values of these constants are now different. We have $A^{\mathrm{sat}}=2-\sqrt{3}$ and $c_1^{\mathrm{sat}}=-j(28+3j-24\sqrt{3})/4$.

C. Comparison between analytical and numerical potential profiles

Gathering results, we obtain up to corrections of order $1/(\kappa a)^2$, $y(r)=y_0(r)+(\kappa a)^{-1}y_1(r)$, where the auxiliary functions y_0 and y_1 are given by Eqs. (2.5) and (2.15) in the 2:1 case, and by Eqs. (2.17) and (2.18) for 1:2 electrolytes. It is instructive to compare the resulting predictions to the numerical solution of Poisson-Boltzmann theory, obtained following the method of Ref. [16]. Figures 1 and 2 show that already for $\kappa a=2$, the agreement is good. Although the potential at contact $y(a)$ is predicted accurately, we observe that our theoretical expression slightly underestimates the potential. A similar trend will be observed for effective

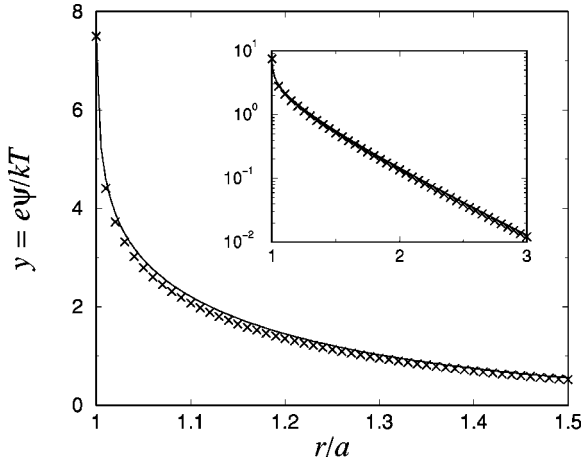

FIG. 1. Reduced electrostatic potential $y(r)$ as a function of rescaled distance for a spherical macroion in a 1:2 electrolyte. The continuous curve shows the numerical solution of the problem, and the crosses indicate the values found from Eqs. (2.17) and (2.18). The inset shows the same data on a linear-log scale. Here, $\kappa a=2$ and the reduced bare charge is very high: $Z_{\mathrm{bare}} l_B/a=2000$.

charges—again for spheres—in Sec. III. In cylindrical geometry, a slight overestimation may be found in the 1:2 case.

The parameters in Figs. 1 and 2 are chosen to be in the nonlinear saturation regime $Z_{\mathrm{bare}} \gg a/l_B$. It is interesting to notice that the relative error of our analytic solution from the numerical one in the cases presented in Figs. 1 and 2 is of order 3%, that is of order $(\kappa a)^{-2}/10$. We have also studied the linear regime, Z_{bare} small, and in this case the error is of larger order, 25%, i.e., of order $(\kappa a)^{-2}$ [remember that in our analytical solution we neglect terms of order $(\kappa a)^{-2}$]. We have also computed the relative error for other values of κa, and the trend is general: in the linear regime the relative error is of order $(\kappa a)^{-2}$, but for the nonlinear saturation regime the situation improves and the error is reduced by a factor of 10. This makes our analytic solution practical since experimental situations are often in the saturation regime where our solution is more accurate.

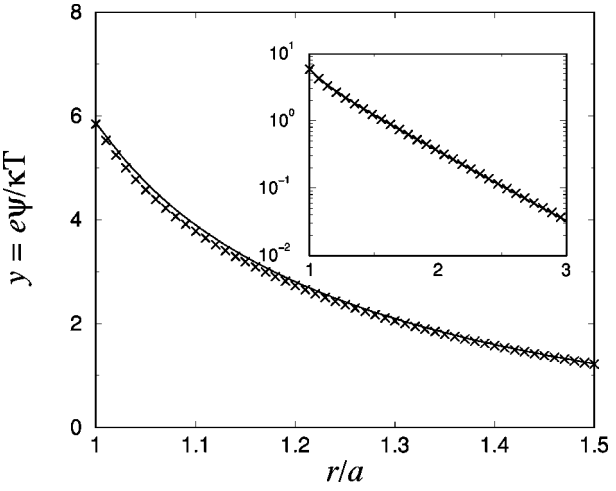

FIG. 2. Same as Fig. 1 in a 2:1 electrolyte. Here, $\kappa a=2$ and the reduced bare charge is $Z_{\mathrm{bare}} l_B/a=34$.

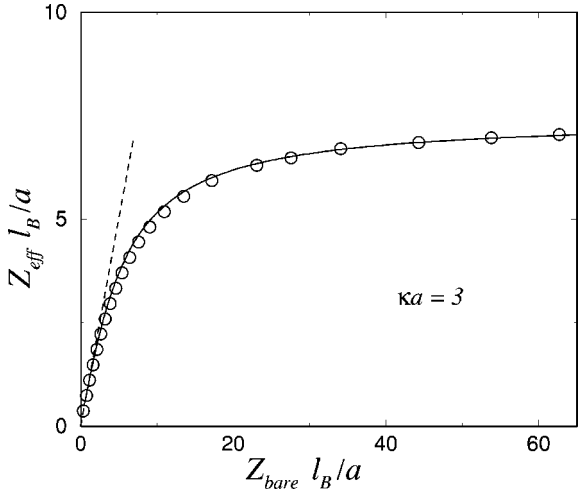

FIG. 3. Effective vs bare charge for a spherical macroion in a 1:2 electrolyte (i.e., monovalent coions/divalent counterions). The open circles are obtained from the full, nonlinear Poisson-Boltzmann theory, while the continuous curve corresponds to the analytical prediction given by Eq. (3.3). The dashed line has slope 1 and shows the initial linear regime for weak charges. The salinity conditions here are such that $\kappa a=3$, where a is the sphere radius.

III. EFFECTIVE CHARGES

A. Spheres

The far-field $r\to\infty$ behavior of the solution $y(r)=y_0(r)+\epsilon y_1(r)+O(\epsilon^2)$, obtained in the last section, is

$$y(r) \underset{r\to\infty}{\sim} A e^{-\kappa(r-a)} \left(\frac{a}{r}\right)^{j/2} \left(6+\frac{c_1}{\kappa a}\right) + O(\epsilon^2). \tag{3.1}$$

With this expression, we can deduce the effective charge. For a spherical macroion ($j=2$) of radius a and charge Z_{eff}, the solution of linearized Poisson-Boltzmann theory (also referred to as Debye-Hückel theory) $\nabla^2 y=\kappa^2 y$ reads

$$y(r) = \frac{Z_{\mathrm{eff}} l_B}{1+\kappa a} \frac{e^{-\kappa(r-a)}}{r}. \tag{3.2}$$

By comparison with expression (3.1), we conclude that the effective charge is given by

$$Z_{\mathrm{eff}} \frac{l_B}{a} = A\left[6\kappa a + 6 + c_1 + O\left(\frac{1}{\kappa a}\right)\right]. \tag{3.3}$$

The coefficients A and c_1 are given by Eqs. (2.10) and (2.16) (2:1 electrolyte) or Eqs. (2.19) and (2.21) (1:2 electrolyte) in terms of the bare charge Z_{bare} by substituting $s=\epsilon Z_{\mathrm{bare}} l_B/a$. Figures 3 and 4 compare the above analytical predictions to the effective charge obtained from the far-field behavior of the numerical solution of Poisson-Boltzmann theory, obtained as explained in Ref. [16]. The agreement is satisfying, and improves upon increasing κa, as was anticipated.

One may readily check from Eq. (3.3) that in the limit $Z_{\mathrm{bare}}\to 0$, $Z_{\mathrm{eff}}/Z_{\mathrm{bare}}\to 1$. Effective and bare parameters coincide in the weak coupling limit, as they should (see the dashed lines in Figs. 3 and 4). In the other limit, where $Z_{\mathrm{bare}}\to\infty$, we observe the saturation picture common to sev-

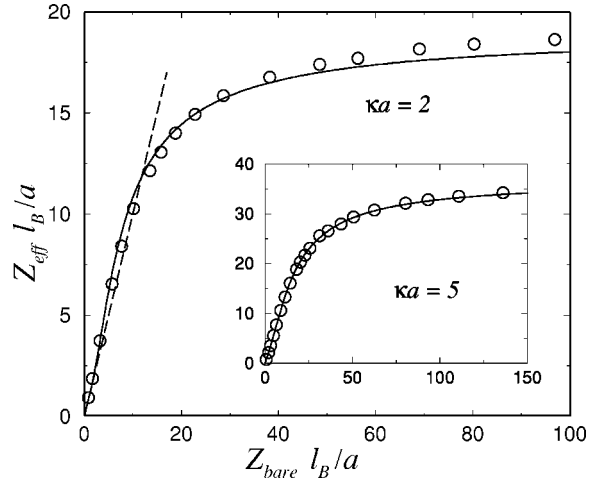

FIG. 4. Same as Fig. 3 for a 2:1 electrolyte (divalent coions, monovalent counterions). As indicated, the main graph corresponds to $\kappa a=2$, while the inset shows results for $\kappa a=5$.

eral mean-field theories [8,11]: the effective charge goes to a plateau value that only depends on two dimensionless quantities, a/l_B and κa. The effective charge at saturation (obtained when $s\to\infty$) takes a simple expression. For a 2:1 electrolyte

$$Z_{\rm eff}^{\rm sat}\frac{l_B}{a}=6\kappa a+7+O\left(\frac{1}{\kappa a}\right), \tag{3.4}$$

and for a 1:2 electrolyte

$$Z_{\rm eff}^{\rm sat}\frac{l_B}{a}=(2-\sqrt{3})[6\kappa a-11+12\sqrt{3}+O(\epsilon)]$$

$$\simeq 1.608\kappa a+2.623+O\left(\frac{1}{\kappa a}\right). \tag{3.5}$$

We note that the conditions of Fig. 1 are those of saturation.

These expressions are tested against the numerical data in Figs. 5 and 6. The agreement is good for $\kappa a>1$. In Figs.5 and 6, an inset has been added to show the regime of low-κa values where our approach breaks down. In this limit, the observed divergence of $Z_{\rm eff}^{\rm sat}$ means that the bare charge is no longer renormalized. As happens for monovalent electrolytes [5], the saturated effective charge is a nonmonotonous function of κa that reaches its minimum for $\kappa a\simeq 0.3$. In the latter 1:1 case, we recall for completeness that the asymptotic expansion $Z_{\rm eff}^{\rm sat}l_B/a=4\kappa a+6$ holds for $\kappa a>1$ [12].

B. Cylinders

For an infinitely long cylindrical colloid, $j=1$, with linear charge density $e\lambda$, the far-field solution (3.1) should be compared to the one obtained from Debye-Hückel theory

$$y(r)=\frac{2l_B\lambda_{\rm eff}}{\kappa a}\frac{K_0(\kappa r)}{K_1(\kappa a)}\underset{r\to\infty}{\sim}\frac{2l_B\lambda_{\rm eff}}{\kappa a}\frac{\sqrt{\frac{\pi}{2\kappa a}}e^{-\kappa a}}{K_1(\kappa a)}\left(\frac{a}{r}\right)^{1/2}e^{-\kappa(r-a)}, \tag{3.6}$$

where K_0 and K_1 are modified Bessel functions. We conclude that the effective line charge density is given by

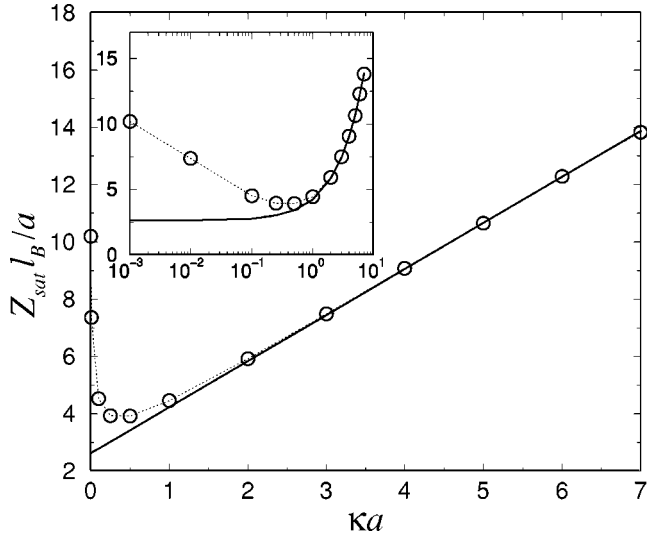

FIG. 5. Effective charge at saturation in a 1:2 electrolyte for a spherical colloid. The line shows the prediction of Eq. (3.5). The circles again correspond to the numerical resolution of Poisson-Boltzmann theory, and the dotted line between them is a guide to the eye. The inset shows the same data in a log-linear scale.

$$\lambda_{\rm eff}l_B=A\left[3\kappa a+\frac{9}{8}+\frac{c_1}{2}+O\left(\frac{1}{\kappa a}\right)\right]. \tag{3.7}$$

The explicit expression of the effective linear charge density in terms of the bare linear charge density $\lambda_{\rm bare}$ is obtained by reporting $s=2\epsilon l_B\lambda_{\rm bare}$ in the analytical expressions for A and c_1 given in Eqs. (2.10) and (2.16) (2:1 electrolyte) or Eqs. (2.19) and (2.21) (1:2 electrolyte). Figure 7 shows the accuracy of our analytical expression, that turns out to be slightly better in the 2:1 situation than in the 1:2 case (the reverse observation follows from inspecting Figs. 5 and 6).

The effective charges at saturation are, for a 2:1 electrolyte

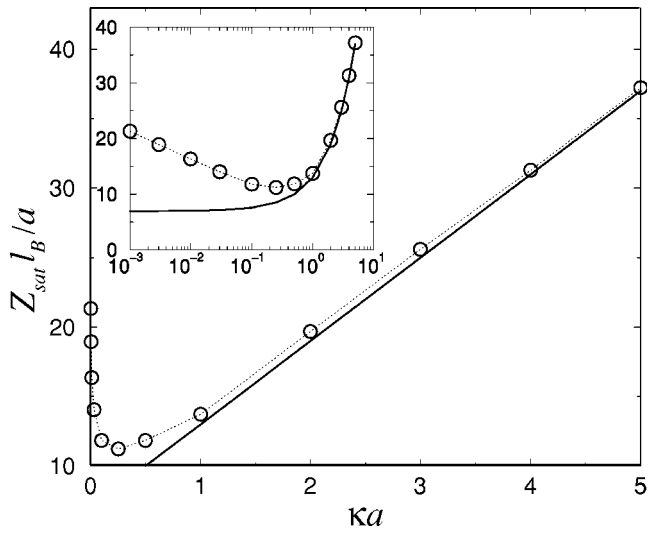

FIG. 6. Same as Fig. 5 for a 2:1 electrolyte. The line shows the prediction of Eq. (3.4).

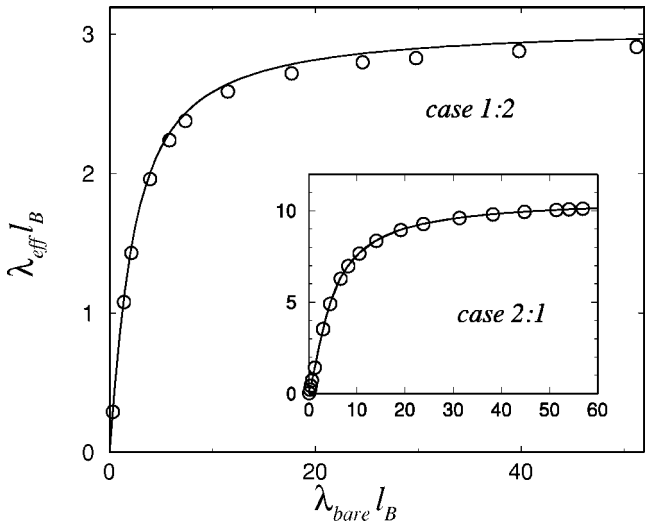

FIG. 7. Effective line charge density as a function of its bare counterpart, for a rod-like macroion. The line shows the prediction of Eq. (3.7) and the symbols stand for the "exact" numerical values. The main graph and the inset correspond to the same salinity conditions $\kappa a = 3$, where a is the cylinder's radius.

$$\lambda_{\rm eff}^{\rm sat} l_B = 3\kappa a + \frac{7}{4} + O\left(\frac{1}{\kappa a}\right), \tag{3.8}$$

and for a 1:2 electrolyte

$$\lambda_{\rm eff}^{\rm sat} l_B = (2-\sqrt{3})\left[3\kappa a - \frac{11}{4} + 3\sqrt{3} + O(\epsilon)\right]$$

$$\simeq 0.804\kappa a + 0.655 + O\left(\frac{1}{\kappa a}\right). \tag{3.9}$$

These simple expressions are plotted in Figs. 8 and 9, together with their counterparts obtained from the solution of Poisson-Boltzmann theory, shown by symbols. When converted into effective surface charge densities $\sigma_{\rm eff}^{\rm sat}$, the previous results yield, up to $(\kappa a)^{-1}$ corrections

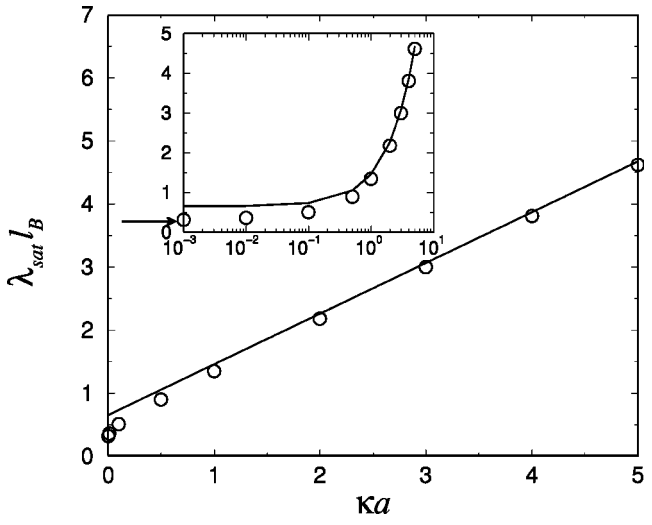

FIG. 8. Saturated effective line charge of an infinite cylinder with radius a in a 1:2 electrolyte. Line: Eq. (3.9) and symbols: numerical solution. The inset is a log-linear plot. The arrow indicates the value $\sqrt{3}/(2\pi) \simeq 0.275$, obtained in the $\kappa a \to 0$ limit [21,22].

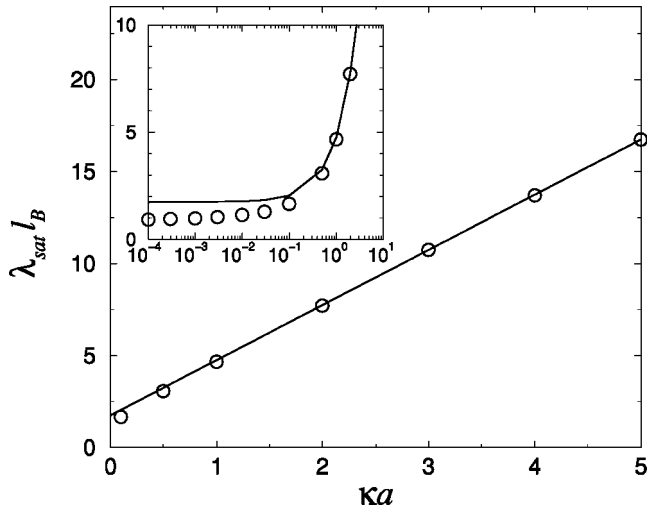

FIG. 9. Same as Fig. 8 for a 2:1 electrolyte. The line corresponds to Eq. (3.8).

$$4\pi a l_B \sigma_{\rm eff}^{\rm sat} = 6\kappa a + 7 \ (2{:}1,\ \text{spheres}) \tag{3.10}$$

$$= 6\kappa a + \frac{7}{2} \ (2{:}1,\ \text{rods}), \tag{3.11}$$

while in the planar case, one gets $4\pi a l_B \sigma_{\rm eff}^{\rm sat} = 6\kappa a + 0$. The increase of the zeroth-order term $(0, 7/2, 7)$ as the dimensionality of the object increases, reflects the concomitant weaker range of the bare Coulomb potential ($-r$ in 1D, $-\log r$ in 2D, $1/r$ in 3D…). Indeed, a weaker Coulomb contribution leads to a weaker screening, hence a higher effective charge. A similar argument therefore explains the increase of effective charges with κa. For completeness, we also give the 1:2 results

$$\frac{4\pi a l_B \sigma_{\rm eff}^{\rm sat}}{(2-\sqrt{3})} = [6\kappa a - 11 + 12\sqrt{3}] \ (\text{spheres}) \tag{3.12}$$

$$= \left[6\kappa a - \frac{11}{2} + 6\sqrt{3}\right] \ (\text{rods}), \tag{3.13}$$

and the same argument as above applies here equally.

It may be observed in Figs. 8 and 9 that in cylindrical geometry, the saturated effective charge does not diverge in the limit $\kappa a \to 0$, as was the case for spheres due to entropic reasons (Boltzmann beats Coulomb in this limit). With infinite cylinders, this is no longer the case (a two-dimensional situation is more favorable to Coulomb than a 3D one), and $\lambda_{\rm eff}^{\rm sat}$ reaches a constant value for small κa (see the inset of Figs. 8 and 9).

C. An overshooting effect

Although the effect is not very marked, it may be observed in Fig. 4 that $Z_{\rm eff}$ as a function $Z_{\rm bare}$ has an inflection

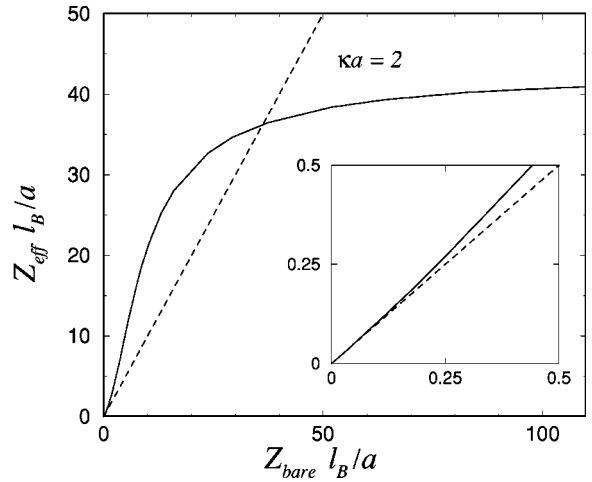

FIG. 10. Illustration of the overshooting effect, for a spherical colloid in a 5:1 electrolyte, with $\kappa a=2$. The dashed line has slope 1 and the inset (a zoom of the bottom left corner) shows that for small charges, Z_{eff} is a convex-up function of Z_{bare}.

point, so that $Z_{\mathrm{eff}}>Z_{\mathrm{bare}}$ in a given charge range ($0<Z_{\mathrm{eff}}<10a/l_B$, where not only our prediction but also the symbols showing numerical data lie above the dashed line). This was unexpected since with a monovalent (1:1) electrolyte, the effective charge is always smaller than the bare one. This overshooting effect occurs for spherical but also for rod-like macroions. It requires a 2:1 salt for which the divalent coions are expelled from the vicinity of the macroion, which leads to a much weaker screening than in the reverse 1:2 situation. That this effect is able to impose $Z_{\mathrm{eff}}>Z_{\mathrm{bare}}$ is however surprising, and in order to check its robustness we also investigated more asymmetric electrolytes numerically. Figure 10 shows that for a 5:1 salt, the overshooting is more pronounced and for $Z_{\mathrm{eff}}\simeq 10a/l_B$, the effective charge may be twice as big as the bare one.

Additional insight into this unexpected overshooting effect may be obtained from our analytical expressions for the effective charges, Eqs. (3.3) and (3.7). For a small surface charge density s, in the 2:1 case, the quantities A and c_1 involved in the expressions of the effective charges have a Taylor expansion of the form

$$A=\frac{s}{6}+\frac{s^2}{18}-\frac{s^3}{216}+O(s^4), \tag{3.14a}$$

$$c_1=-\frac{9}{4}-\frac{7s}{3}+\frac{13s^2}{24}+\frac{10s^3}{9}+O(s^4);\ \text{rods}, \tag{3.14b}$$

$$c_1=-6-\frac{14s}{3}+\frac{13s^2}{12}+\frac{20s^3}{9}+O(s^4);\ \text{spheres}. \tag{3.14c}$$

For rods, this gives the following behavior of the effective linear charge density for small bare charge:

$$\lambda_{\mathrm{eff}}l_B=\lambda_{\mathrm{bare}}l_B+\frac{s^2}{6}\left(\kappa a-\frac{7}{6}\right)-\frac{s^3}{72}\left(\kappa a+\frac{17}{12}\right)+O(s^4). \tag{3.15}$$

In this case $s=2\lambda_{\mathrm{bare}}l_B(\kappa a)^{-1}$. For spherical colloids, the behavior for small bare charges is

$$Z_{\mathrm{eff}}\frac{l_B}{a}=Z_{\mathrm{bare}}\frac{l_B}{a}+\frac{3s^2}{9}\left(\kappa a-\frac{7}{3}\right)-\frac{s^3}{36}\left(\kappa a+\frac{17}{6}\right)+O(s^4), \tag{3.16}$$

now with $s=Z_{\mathrm{bare}}l_B/(\kappa a^2)$. Remembering that our analytical solution is valid for large values of κa, we notice that in both cases the coefficient of the term of order two in the bare surface charge density s is positive. This implies that the effective charge will become larger than the bare charge in a certain intermediate regime of values of the bare charge when nonlinear effects start to become important (being nevertheless far from the strongly nonlinear saturated regime where the effective charge saturates). Let us mention that this overshooting effect is also expected for a planar geometry, since in that case the effective charge is essentially given by A.

In contrast with this, in the case of a 1:2 electrolyte the Taylor expansions of A and c_1 are similar to Eqs. (3.14) with the formal replacement $s\to -s$ and $A\to -A$; in particular, the sign of the order s^2 in A changes sign. This gives the following behavior for the effective charges:

$$\lambda_{\mathrm{eff}}l_B=\lambda_{\mathrm{bare}}l_B-\frac{s^2}{6}\left(\kappa a-\frac{7}{6}\right)-\frac{s^3}{72}\left(\kappa a+\frac{17}{12}\right)+O(s^4) \tag{3.17}$$

for rods, and

$$Z_{\mathrm{eff}}\frac{l_B}{a}=Z_{\mathrm{bare}}\frac{l_B}{a}-\frac{3s^2}{9}\left(\kappa a-\frac{7}{3}\right)-\frac{s^3}{36}\left(\kappa a+\frac{17}{6}\right)+O(s^4) \tag{3.18}$$

for spheres. The coefficient of s^2 has changed sign with respect to the 2:1 case. This coefficient is now negative, and this implies that the effective charge will remain smaller than the bare charge, thus no overshooting effect for the 1:2 electrolyte case.

It is interesting to mention that for a symmetric 1:1 electrolyte, the small bare charge behavior reads [12]

$$\lambda_{\mathrm{eff}}l_B=\lambda_{\mathrm{bare}}l_B-\frac{x_r^3}{4}\left(\kappa a-\frac{1}{4}\right)+O(x_r^5) \tag{3.19}$$

for rods, with $x_r=\lambda_{\mathrm{bare}}l_B/[\kappa a+(1/2)]$ and

$$Z_{\mathrm{eff}}\frac{l_B}{a}=Z_{\mathrm{bare}}\frac{l_B}{a}-\frac{x_s^3}{2}\left(\kappa a-\frac{1}{2}\right)+O(x_s^5) \tag{3.20}$$

for spheres, with $x_s=Z_{\mathrm{bare}}l_B/[2a(\kappa a+1)]$. Interestingly, there is no term of order two in the bare charge as opposed to the asymmetric electrolytes cases. The first correction to the linear term is of order three and it is negative. The effective charge will be smaller than the bare charge: no overshooting effect here either.

The first corrections to the linear theory are of order two in the bare charge for asymmetric electrolytes, with the sign of $\Sigma_\alpha z_\alpha^3 n_\alpha$, z_α being the valency of species α and n_α its density. On the other hand, for symmetric electrolytes, the first correction is of order three in the bare charge. This important difference between symmetric and asymmetric electrolytes also appears in others contexts, namely in the study of the contributions due to correlations to the effective charge, in a framework going beyond the mean-field approximation [17–19].

Finally, we mention that recent HNC integral equation computations for the same systems as investigated here confirm the validity of the overshooting effect [20]. Explicit comparisons with our predictions are under way [20].

IV. COLLOIDS AS CONSTANT POTENTIAL OBJECTS

Colloids are usually highly charged so that their effective charge—within mean field—is saturated and therefore independent of the bare one. Yet, the bare charge is often not large enough to meet the region of high microionic electrostatic correlations where the mean-field approach would break down [7,11]. This has led to the proposal to consider highly charged colloids as objects of fixed effective potential in the case of a 1:1 electrolyte [8]. Similar considerations may be put forward here. From the analysis of Sec. III, the surface potentials $y=e\psi/(kT)$ associated with effective charges read, for spheres

$$y_{\rm eff}^{\rm sat} = 6 + \frac{1}{1+\kappa a};\ (2{:}1),$$
$$y_{\rm eff}^{\rm sat} = 6(2-\sqrt{3}) + (2-\sqrt{3})\frac{12\sqrt{3}-17}{1+\kappa a};\ (1{:}2). \tag{4.1}$$

The important point is that the κa dependence is very weak for $\kappa a > 1$, which reinforces the picture of constant potential objects. One may therefore consider a highly charged sphere as an effective body of potential $6kT/e$ or $6(2-\sqrt{3})kT/e$ depending on 2:1 or 1:2 asymmetry, irrespective of physicochemical parameters. In a 1:1 salt, one gets a value $4kT/e$ [8]. It is natural to find this quantity in between the two bounds $6kT/e$ and $6(2-\sqrt{3})kT/e$, since screening is all the more efficient as the valency of counterions is large and the valency of coions is low (in absolute values).

For rod-like polyions, we get

$$y_{\rm eff}^{\rm sat} = \left(6 + \frac{7}{2\kappa a}\right)\frac{K_0(\kappa a)}{K_1(\kappa a)};\ (2{:}1),$$
$$y_{\rm eff}^{\rm sat} = \left(6(2-\sqrt{3}) + (2-\sqrt{3})\frac{6\sqrt{3}-11/2}{\kappa a}\right)\frac{K_0(\kappa a)}{K_1(\kappa a)};\ (1{:}2). \tag{4.2}$$

Expressions (4.1) and (4.2) are plotted in Fig. 11.

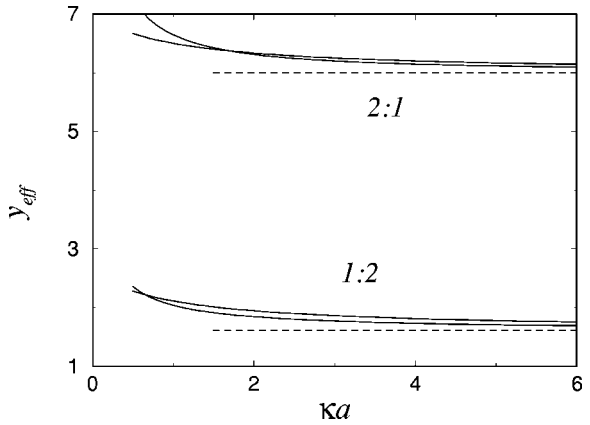

FIG. 11. Effective potentials at saturation following from Eqs. (4.1) and (4.2), as a function of κa. The limiting values for $\kappa a \to \infty$ are shown by the dotted lines.

V. CONCLUSION

In conclusion, we have found an analytical solution of cylindrical and spherical Poisson-Boltzmann equation in asymmetric 1:2 and 2:1 electrolytes. Our approach amounts to performing a curvature expansion, and neglects corrections of order $1/(\kappa a)^2$ for the electrostatic potential. For $\kappa a > 1$, the corresponding solution and associated effective charge are in excellent agreement with their counterparts obtained from the full numerical resolution of the problem.

Our multiple scale analysis relies on the possibility to solve analytically the planar problem (corresponding to $\kappa a \to \infty$). Since for a $n{:}m$ electrolyte (where n and m, respectively, stand for the valency of coions and counterions), this solution is only known explicitly for $n/m = 1, 1/2$, and 2, we focused on 1:2 and 2:1 salts. The monovalent 1:1 situation has been investigated in Refs. [12,13]. For a given salinity κ, nonlinear screening is more efficient with divalent than with monovalent counterions. Accordingly, we always found higher effective charges in the 2:1 than in the 1:2 situation. Surprisingly, we found that 2:1 screening is even able to drive the effective charge in a regime where it is higher than the bare one. This overshooting effect happens in an intermediate charge range, since when $Z_{\rm bare}$ is large enough, $Z_{\rm eff}$ saturates. We finally emphasize that we have worked here within the Poisson-Boltzmann mean-field framework that neglects microionic correlations. For a discussion of the validity of such a picture, we refer to Sec. 7 of Ref. [7], and to the concluding section of Ref. [11].

ACKNOWLEDGMENTS

We thank L. Bocquet, Y. Levin, and M. Aubouy for useful discussions. This work was supported by an ECOS Nord/COLCIENCIAS-ICETEX-ICFES action of French and Colombian cooperation. G.T. acknowledges partial financial support from COLCIENCIAS under Project No. 1204-05-13625.

[1] G. L. Gouy, J. Phys. **9**, 457 (1910).
[2] D. L. Chapman, Philos. Mag. **25**, 475 (1913).
[3] P. Debye and E. Hückel, Phys. Z. **24**, 185 (1923).
[4] See, e.g., E. J. W. Verwey and J. Th. G. Overbeek, *Theory of the Stability of Lyophobic Colloids* (Elsevier, New York, 1948); Dover paperback republication (1999).
[5] L. Belloni, Colloids Surf., A **140**, 227 (1998).
[6] J.-P. Hansen and H. Löwen, Annu. Rev. Phys. Chem. **51**, 209 (2000).
[7] Y. Levin, Rep. Prog. Phys. **65**, 1577 (2002).
[8] E. Trizac, L. Bocquet, and M. Aubouy, Phys. Rev. Lett. **89**, 248301 (2002).
[9] L. Bocquet, E. Trizac, and M. Aubouy, J. Chem. Phys. **117**, 8138 (2002).
[10] We will, however, report here some situations where $|Z_{\text{eff}}| > |Z_{\text{bare}}|$.
[11] G. Téllez and E. Trizac, Phys. Rev. E **68**, 061401 (2003).
[12] M. Aubouy, E. Trizac, and L. Bocquet, J. Phys. A **36**, 5835 (2003).
[13] I. A. Shkel, O. V. Tsodikov, and M. T. Record, J. Phys. Chem. B **104**, 5161 (2000).
[14] D. C. Grahame, J. Chem. Phys. **21**, 1054 (1953).
[15] J. Ulander, H. Greberg, and R. Kjellander, J. Chem. Phys. **115** 7144 (2001).
[16] E. Trizac, L. Bocquet, M. Aubouy, and H. H. von Grünberg, Langmuir **19**, 4027 (2003).
[17] J.-N. Aqua and F. Cornu, Phys. Rev. E **68**, 026133 (2003).
[18] J.-N. Aqua and F. Cornu (unpublished).
[19] G. Téllez, e-print cond-mat/0401475.
[20] D. Levesque (private communication).
[21] C. A. Tracy and H. Widom, Physica A **244**, 402 (1997).
[22] G. Tëllez and E. Trizac (unpublished).